Review Of Research
Vol. 4 | Issue. 3 | Dec. 2014
Impact Factor : 2.1002 (UIF)
ISSN:-2249-894X
Available online at www.lbp.world

ORIGINAL ARTICLE

STRUCTURAL CHARACTERIZATION OF $Y_{3-x}EU_xFE_5O_{12}$ (X= 0.0 TO 0.5) SYSTEM

Shesherao S. Jawale
Department of Electronics, Yeshwantrao Chavan Mahavidyalaya, Tuljapur,
Dist-Osmanabad- 413 601, Maharashtra, INDIA.
Corresponding author: drssjawalepatil@gmail.com

ABSTRACT:

Samples of $Y_{3-X}Eu_XFe_5O_{12}$ (x= 0.0 to 0.5) were prepared by using high purity Y_2O_3, Eu_2O_3, Fe_2O_3 and using ceramic technique. Powder X-ray diffractograms (XRD pattern) for all the samples were recorded at room temperature. All the samples of the series $Y_{3-x}Eu_xFe_5O_{12}$ synthesized by ceramic technique possesses single-phase cubic garnet structure, which is evidenced by X-ray diffraction data. The cation distribution of the present garnet system suggest that Eu^{3+} occupies dodecahedral (C) site and is in agreement with that of other garnet system.

KEYWORDS: Yttrium iron garnet (YIG), $Y_{3-x}Eu_xFe_5O_{12}$, cation distribution

INTRODUCTION:

Yttrium Iron Garnet (YIG) and substituted YIG have been investigated extensively because of their technical importance and the ease with which properties can be tailor made to suit various applications [1-4]. Number of ions can be substituted in YIG which occupy the lattice site determined primarily by their ionic radii [3]. It is found that certain ions occupy strictly a particular lattice sites while some others can occupy both tetrahedral (d) and octahedral [a] sites present in YIG structure [5, 6]. Substituted rare earth iron garnets show wide variety of interesting magnetic properties [1, 5]. Theoretical models, one based on Neel's model [7], another suggested by de-Geenes [8] based on Yafet-Kittel models [9], and one suggested by Gilleo [10] have been used to explain the magnetic behaviour of YIG.

Yttrium iron garnet (YIG) is a cubic crystal (space group Ia^3d-O_h^{10}) characterized by following structural-chemical formula

$$[Y_3]^C, [Fe_3^{3+}]. [Fe_2^{3+}]^a. [O\frac{2-}{12}]$$

The trivalent iron cations are distributed over two different sets of lattice sites; octahedral (a) and tetrahedral (d) sub-lattice in which each cations is tetrahedrally surrounded by oxygen anions and on octahedral (a) sub-lattice where the co-ordination is octahedral. The yttrium ions are in dodecahedra (C) sites characterized by a dodecahedral oxygen environment.

A large number of cations can be substituted at yttrium sites or at iron (Fe^{3+}) sites enabling a wide variation in the properties of garnets. The magnetic properties of gallium and aluminum [10, 11] substituted yttrium iron garnet have been reported in the literature [11]. Similarly, the structural, electrical and magnetic properties of non-magnetic Si and Ge substituted YIG, have also been reported in the literature [12, 13].

In the literature, studies on the properties of pure yttrium iron garnet [14], and pure europium iron garnet [15] have been reported in the literature on the structural, electrical, magnetic properties of europium substituted yttrium iron garnet.

Since Yttrium is non-magnetic whereas europium is a magnetic having magnetic moment .74 μB , Therefore, it will be interesting to see the effect of substitution of magnetic Eu^{3+} ions in the lattice of pure yttrium iron garnet at yttrium site.

In the present work, the structural characterization of all the samples of the series $Y_{3-X}EU_XFe_5O_{12}$ (X= 0.0 to 0.5) were done by x-ray diffraction technique.

EXPERIMENTAL:

Samples of $Y_{3-X}Eu_XFe_5O_{12}$ (X= 0.0 to 0.5) were prepared by using high purity Y_2O_3, Eu_2O_3, Fe_2O_3 and using ceramic technique. The oxides were mixed thoroughly in stoichiometric proportions to yield the desired composition and wet ground. The mixture was dried and presintered at 1050^0C for 24 hours in air and cooled to room temperature. The powder was reground and pelletized using hydraulic press. The cylindrical pellets were finally sintered at 1350^0C for 24 hours and slowly cooled to room temperature at the rate of 2^0C per minute to obtain garnet phase.

The powder X-ray diffractograms (XRD pattern) for all the samples were recorded at room temperate (Model PW-3710). XRD patterns were obtained in the 2θ range of 20^0 to 80^0 and using C_r-Kα radiation.

RESULT AND DISCUSSION:

X-ray powdered diffraction patterns of the series $Y_{3-x}Eu_xFe_5O_{12}$ with X = 0.0 to 0.5 are shown in Fig. 4.1 and Fig. 4.2. XRD patterns indicated that the materials formed in a single phase with a cubic garnet structure. All the peaks of the XRD patterns (d) for the recorded peak were calculated according to Bragg's law for all the composition under investigation. The values of inter-planer spacing 'd' for different (hkl) are listed in Table 4.1.

Table 4.1: Miller indices (hkl) and inter-planer spacing (d) for $Y_{3-x}Eu_xFe_5O_{12}$ system (x = 0.0 to 0.5)

Plane (hkl)	Inter-planer spacing 'd' (Å)					
	x=0.0	x=0.1	x=0.2	x=0.3	x=0.4	x=0.5
(400)	4.009	4.006	4.010	4.002	3.999	4.005
(331)	4.417	4.418	4.427	4.423	4.417	4.417
(420)	4.471	4.502	4.408	4.475	4.468	4.476
(422)	4.905	4.909	4.910	4.904	4.899	4.889
(440)	5.699	5.698	5.702	5.697	5.689	5.688
(622)	6.643	6.645	6.644	6.639	6.633	6.630
(640)	7.228	7.225	7.223	7.223	7.220	7.219
(642)	7.500	7.509	7.499	7.491	7.489	7.485

The XRD data was used to evaluate unit cell dimensions. The lattice constant 'a' was determined using the fallowing relation,

$$A=d\sqrt{N} \qquad \textbf{(4.1)}$$

Where,

d is inter-planer spacing

N is $(h^2+k^2+l^2)$, (hk1) are Miller indices

The values of lattice constant 'a' determined from XRD data with an accuracy of $\pm$ 0.002Å are given in Table 4.2.

Table 4.2 : Lattice constant (a), particle size (t) and theoretical lattice constant (a_{th}) for $Y_{3-x}Eu_xFe_5O_{12}$ system (x = 0.0 to 0.5)

Composition 'x'	Lattice constent 'a' (Å)		Particle size 't' (Å)
	Obs.	The	
0.0	12.334	12.322	152
0.1	12.331	12.325	151
0.2	12.328	12.329	151
0.3	12.338	12.332	151
0.4	12.349	12.336	151
0.5	12.349	12.339	151

The variation of lattice constant with composition has been studied. Fig.4.3 depicts the variation of lattice constant 'a' with Eu substitution. It is observed from Fig.4.3 that

lattice constant increases with Eu substitution. The lattice constant increases linearly and obeys Vegard's law [17]. The increasing behavior of lattice constant with Eu substitution can be understood from the knowledge of ionic radii of the constituent ions. In the present series of garnet ($Y_{3-X}Eu_XFe_5O_{12}$), yttrium ions of smaller ionic radii (0.89 Å) are replaced by Eu^{3+} of larger ionic radii (0.95 Å) and therefore lattice constant of present garnet system increases with Eu substitution. Similar behaviour of lattice constant with composition 'x' was observed in ($Y_{3-X}Eu_XFe_5O_{12}$) [18].

The XRD line width and particle size are connected through the Scherrer equation [19]

$$t = \frac{0.9\lambda}{B\cos\theta B} \qquad \textbf{(4.2)}$$

Where,

t is particle diameter,

λ is the wavelength and

B is a measure of the broadening of diffraction line due to size effect.

The values of particle size obtained from above relation are summarized in Table 4.2. It is clear from Table 4.2 that all the samples have almost same particle size.

The X-ray density of all the samples of the series $Y_{3-X}EU_XFe_5O_{12}$have been calculated from the molecular weight and volume of the unit cell using the formula,

$$d_x = \frac{8\,M}{Na3}\ \text{gm. Cm}^3 \qquad \textbf{(4.3)}$$

Where,

M is the molecular weight,

N is the Avogadro's number and

a is the lattice constant.

The values of X-ray density are listed in Table 4.3. It is observed from Table 4.3 that X-ray density increases with increase in Eu substitution.

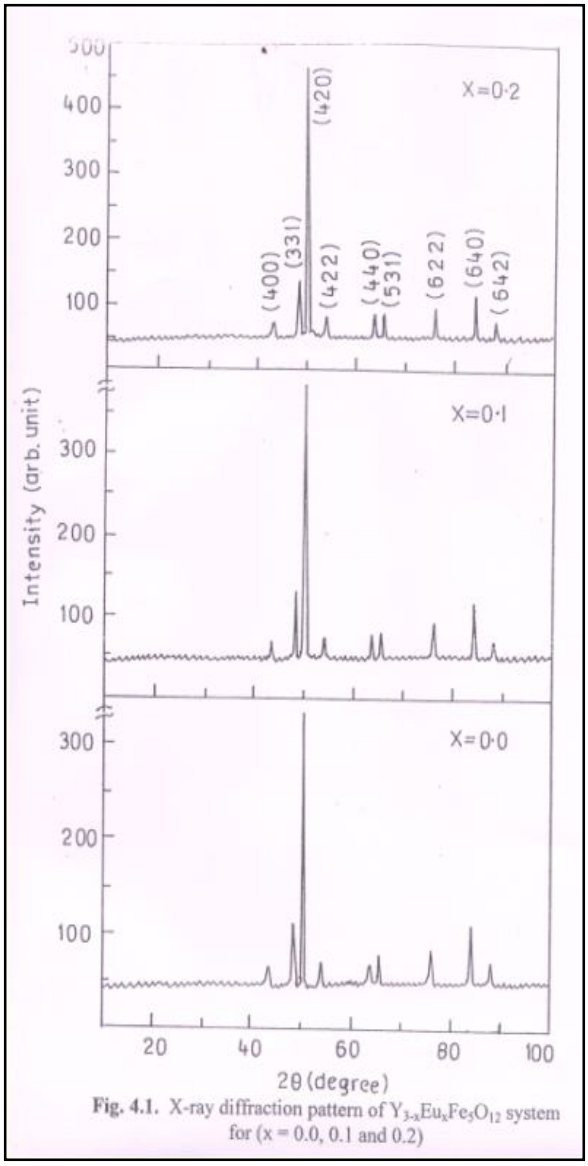

Fig. 4.1. X-ray diffraction pattern of $Y_{3-x}Eu_xFe_5O_{12}$ system for (x = 0.0, 0.1 and 0.2)

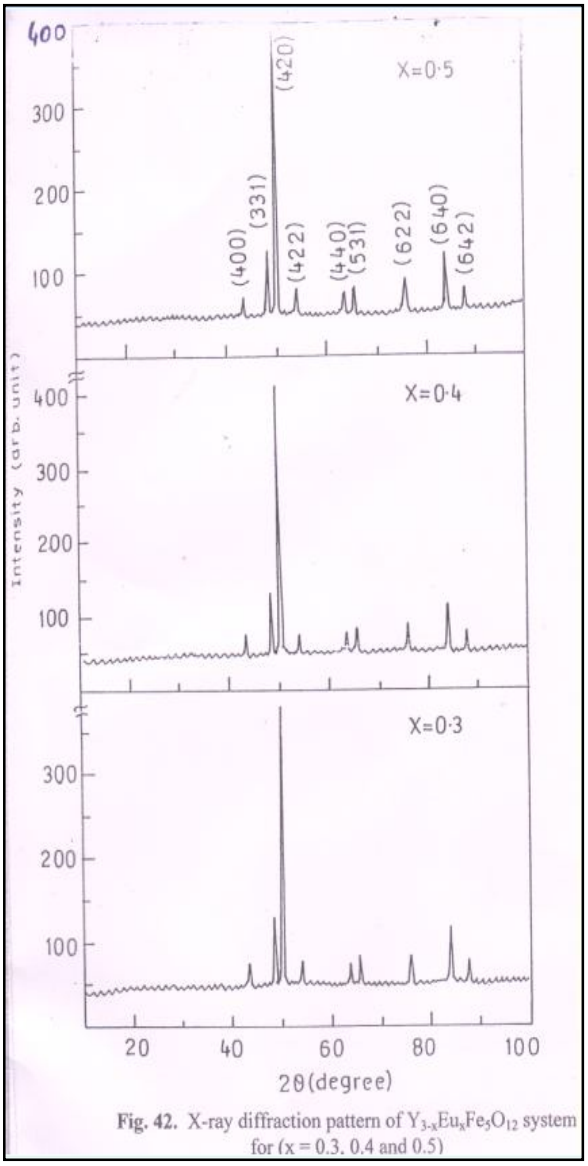

Fig. 42. X-ray diffraction pattern of $Y_{3-x}Eu_xFe_5O_{12}$ system for (x = 0.3, 0.4 and 0.5)

Table 4.3: Molecular weight (M), X-ray density (d_x), Bulk density (d) and porosity for $Y_{3-x}Eu_xFe_5O_{12}$ system (x = 0.0 to 0.5)

Composition 'x'	Mol. Wt. M (gm)	X-ray density 'd_x' (g/cm^3)	Bulk Density 'd' (g/cm^3)	Porosity 'p' %
0.0	738	5.222	5.339	2.23
0.1	744	5.272	5.193	1.5
0.2	751	5.318	5.092	4.2
0.3	757	5.350	5.172	3.3
0.4	763	5.380	5.176	3.81
0.5	769	5.425	5.382	0.80

The variation of X-ray density with composition 'x' is shown in Fig.4.4. It is clear from Fig.4.4 that X-ray density increases with increase in Eu substitution.

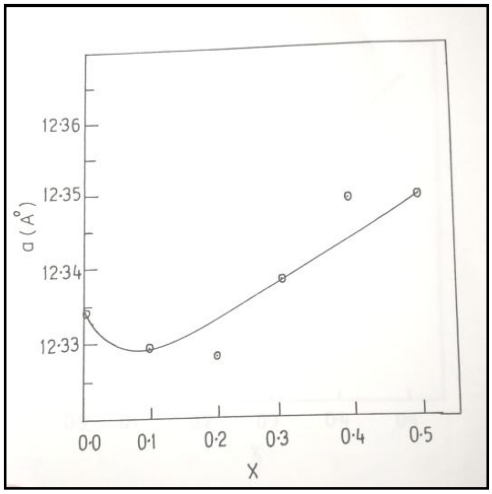

Fig. 4. 3. Variation of lattice parameter 'a' with composition (x= 0.0 – 0.5) for $Y_{3-x}Eu_xFe_5O_{12}$ system

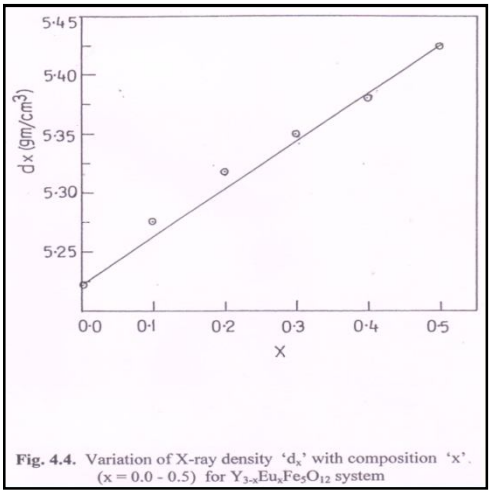

Fig. 4.4. Variation of X-ray density 'd_x' with composition 'x'. (x = 0.0 - 0.5) for $Y_{3-x}Eu_xFe_5O_{12}$ system

In the present series $Y_{3-X}Eu_XFe_5O_{12}$, the lattice constant increases with Eu substitution. Therefore, naturally the X-ray density should decrease. However, in the present study X-ray density increases instead of decreasing. This is because of the fact that the increase in mass overtakes the increase in volume of the unit cell. The values of the molecular weight of all the samples of the series $Y_{3-X}Eu_XFe_5O_{12}$ are given in the Table4.3. The bulk density of the all the samples of the series $Y_{3-X}Eu_XFe_5O_{12}$ was obtained using the values of mass and dimensions of the pellets. The values of bulk density are presented in Table 4.3.

From Table 4.3 it is clear that the bulk density is of the order of 95% to that of X-ray density.

The percentage porosity (P) of all the samples was calculated using the relation

$$P = \left(1 - \frac{d}{dx}\right) \times 100\ \% \qquad \textbf{(4.4)}$$

Where,
d is bulk density
dx is X-ray density
The values of porosity of all the samples are listed in Table 4.3. The porosity values indicate that the samples are dense and compact.

CATION DISTRIBUTION

The study of the distribution of cations among the available sites in ferrites is very much important in understanding the structural and magnetic behaviour of ferrite. The

cation distribution can be obtained from X-ray distribution [20], Mossbauer spectroscopy [21], neutron diffraction [22] and magnetization method [23].

In garnet cations are distributed at three sub-lattices namely dodecahedral (c), octahedral (a) and tetrahedral (d). The total magnetic moments on the 'a' and 'd' ions are aligned anti-parallel and moments on the 'c' ions are anti-parallel to those on the 'd' ion. Thus for the formula $(3M_2O_3)^c\ (2Fe_2O_3)^a\ (3Fe_2O_3)^d$ the arrangement is $6Fe^d$, $4Fe^a$, $6M^c$. The net moment m (in Bohr magnetons per unit formula) is

$$M= 6m_c- (6m_d-4m_a) =6m_c-10\mu_B \quad \textbf{(4.5)}$$

Assuming a moment of $5\mu_B$ per Fe ion. In terms of the unit formula $M_3Fe_2Fe_3O_{12}$ eq. (4.5) becomes

$$M=3m_c-5\mu_B \quad \textbf{(4.6)}$$

In general, the cation distribution of yttrium iron garnet is expressed as,

$$\{Y_3\}^a\ [Fe_2]^a\ (Fe_3)^d\ O_{12} \quad \textbf{(4.7)}$$

Comparing the site preference energy of the constituent ions and assuming that Eu^{3+} has tendency to occupy dodecahedral C-sites, the cation distribution of the present garnet system

$Y_{3-x}Eu_x\ Fe_5^{\ d}\ O_{12}$ can be written as,

$$\{Y_{3-x}Eu_x\}^c\ [Fe_2]^a\ (Fe_3)^d\ O_{12} \quad \textbf{(4.8)}$$

The average ionic radius of dodecahedral (c), octahedral (a) and tetrahedral (d) can be estimated using the relation [24]

$$r_d = [x\ (Fe^{3+}).\ r\ (Fe^{3+})] \quad \textbf{(4.9)}$$

$$r_a = {}^1/_2\ [(xFe^{3+}).\ r\ (Fe^{3+}) +x\ (Fe^{2+}).r\ (Fe^{2+})] \quad \textbf{(4.10)}$$

$$r_c = [x(Y^{3+}).r\ (Y^{3+}) +x\ (Fe^{3+}).r\ (Fe^{2+})] \quad \textbf{(4.11)}$$

Were, x and r represents concentration and ionic radius of cations on the respective sites. Using above equations (4.9, 4.10 and 4.11), considering the ionic radii of yttrium (Y^{3+}) as (0.89Å), Europium Eu^{3+} (0.95 Å) and ferric (Fe^{3+}) as (0.64Å) and the cation distribution formula given by eq. 4.8, the radius of dodecahedral (c), octahedral (a) and tetrahedral (d) were calculated and the values were summarized in Table 4.4.

Table 4.4
Ionic radii of dodecahedral (r_c), octahedral (r_a), tetrahedral (r_d) sites and average radius for $Y_{3-x}Eu_xFe_5O_{12}$ system (x = 0.0 to 0.5)

Composition 'x'	r_c (Å)	r_a (Å)	r_d (Å)	Average radius (Å)
0.0	0.890	0.640	0.640	0.723
0.1	0.892	0.640	0.640	0.724
0.2	0.894	0.640	0.640	0.725
0.3	0.896	0.640	0.640	0.725
0.4	0.898	0.640	0.640	0.726
0.5	0.900	0.640	0.640	0.727

The theoretical lattice constant of all the samples were also estimated using the formula [25],

$$a_{th} = b_1+b_2r_c+b_3r_d+b4r_cr_d+b_6r_cr_a \qquad \textbf{(4.12)}$$

Were, $b_1 - b_6$ are exchange interaction in agreement with earlier report [26].

The values of theoretically obtained lattice constant are given in the Table 4.2 It is observed from Table 4.2 that the theoretical and experimental values of lattice constant are in good agreement, which indirectly suggest that assumed cation distribution is correct. The values of theoretical and experimental lattice constant are in good agreement.

CONCLUSION:

All the samples of the series $Y_{3-x}Eu_xFe_5O_{12}$ synthesized by ceramic technique possesses single-phase cubic garnet structure, which is evidenced by X-ray diffraction data. The lattice parameter of pure YIG is in good agreement with the reported data [27]. The lattice constant increases with Eu substitution. The cation distribution of the present garnet system suggest that Eu^{3+} occupies dodecahedral (C) site and is in agreement with that of other garnet system (28).

ACKNOWLEDGEMENT:

The author is thankful to Prof. Dr. K. M. Jadhav, Department of Physics, Dr. Babasaheb Ambedkar Marathwada University, Aurangabad for his guidance and support.

REFERENCES

[1] Geller s. , Williams H. J. , Espinosa G. P. and Sherwood R. C ., Bell System Tech. J. 43 (1964) 565.
[2] Wilhem H. , von Aulock, "Handbook of microwave ferrite materials", Academic press Inc. (London) 1965
[3] Pauthnet R. , CR Acad Sci. 243 (1956) 1499
[4] Geller S. , Williams H. J. amd Sherwood R. C. , Phys. Rev. 123 (1961) 1692
[5] Geller S. , J. Appl. Phys. 31 (196) 305.
[6] Espinosa G. P. , Inorg. Chem 3 (1964) 848.

[7] Neel L. , Ann. Phys (paris) 3 (1948) 137.
[8] P. G. de Gennes, Phys. Rev. Letters 3 (1959) 209.
[9] Yafet Y. and kittel C. , Phy. Rev. 87 (1952) 290.
[10] Gilleo M. A. , phys-chem. Solids. , 13 (1960) 33.
[11] Gilleo M. A. , J. phys. Chem. Solids 13 (1960) 33.
[12] Geller S. , J. Appl. Phys 37 (1966) 1408.
[13] Geller S. , J. Appl. Phys. Suppl. 31 (1968) 5.
[14] Pauthendt R. , J. Appl. Phys. Suppl. 30 (1968) 4.
[15] Nowik I. And ofer S. Phys. Rev. 153 (1967) 409
[16] Radhakrishnamurthy C. and Likhite S. D. Eae plant sci. Lett. 7 (1970) 389.
[17]Radhakrishnamurthy C. and Likhite S. D. and Sahastrabudhe P. W. , Ind. Acad. Sci. 87 (a) (1978) 245.
[18] R. P. vara, H. J. Shah, M. P. pandya, M. C. chahantbar and k. B. Modi Ind. J. pure. Appl. Phys 42 (2004) 117
[19] Cullity B. D., "Elements of X-ray Diffraction"(Addition Wesley Public Inc. Reading, mass) (1956).
[20] D. S. Birajdar, Devatwal U. N. and Jadhav K. M J. Mater. Sci. 37 (2002) 1443
[21] Jani N. N. Trivedi B. S., Joshi H. H. Bichile G. K. and Kulkarni R. G., Bull. Mater. Sci 21 (1998) 639
[22] A. K. Ghatge, S. A. Patil S. K. Parangpe, Sil. State Commun. 98 (1996) 885
[23] A. M. Shaikh, S. C. Watawe, S. S. Bellad, S. A. Jadhav, B. K. Chougule Mat. Chem. and Phys. 65 (2000) 46
[24] Shannon R. D. and Orewitt C. T., Acta. Cryst. B 25 (1969) B 20 (1970)
[25] Sung Ha Lee, Kwang Pyo Chae, Seok Won Hong and Yound Bae Lee Solid state Comm. 83 (1992) 97.
[26] Tebble R. S. and Craik D. J. "Magnetic materials" John Wiley (London)
[27] Standley K. J., "Oxide Magnetic materials" Carendon Press Oxford (1962).
[28] Murumkar V. D., Modi K. B., Jadhav K. M., Bichile G. K. and Kulkarni R. G., Matt. Lett. 32 (1997) 281